Z. Phys. A 358, 207–211 (1997)

ZEITSCHRIFT
FÜR PHYSIK A

From discrete rotational bands to damped rotational motion

E. Vigezzi[1], **T. Døssing**[2], **M. Matsuo**[3], **K. Yoshida**[3], **P. Bosetti**[1,4], **A.Bracco**[1,4], **S. Frattini**[1,4], **B. Herskind**[2], **S. Leoni**[1,2]

[1] INFN, Sezione di Milano, Via Celoria 16, I-20133 Milano, Italy
[2] The Niels Bohr Institute, University of Copenhagen, Copenhagen, Denmark
[3] Yukawa Institute for Theoretical Physics, Kyoto University, Kyoto 606-01, Japan
[4] Dipartimento di Fisica, Università di Milano, Via Celoria 16, I-20133 Milano, Italy

Received: 8 September 1996
Communicated by B. Herskind

Abstract. We present shell model calculations for warm rotating nuclei, combining the cranked Nilsson mean field and a residual surface-delta two-body interaction. The model is used to describe the transition from the region of well-defined rotational bands into the region dominated by rotational damping, and the results are in overall agreement with the experimental findings.

PACS: 21.10.Re; 21.10.Tg; 23.20.En; 27.60.+j

1 Introduction

There is evidence that in warm, rotating nuclei the rotational degree of freedom is damped, in the sense that a given inital state can populate many final states. This is in contrast to the region close to yrast, where the decay goes to one final state along a well defined rotational band [1, 2]. The mean field states, on which rotational bands are built, react in a different way to the rotation, so that at a given spin I they display a distribution of transition energies E_γ, or frequencies $\omega = E_\gamma/2$, whose width is denoted by Γ_ω. The phenomenon of rotational damping takes place because, when the level density becomes sufficiently high, the mean field states are mixed by the residual interaction, and acquire a spreading width Γ_μ; the decay of each resulting compound state then can reflect the distribution of frequencies of the admixed mean field states. If it can be assumed that the mixed states behave according to the general statistical theory of random matrices, it is possible to obtain simple expressions for the strength function of the damped rotational motion and for its width, the rotational damping width Γ_{rot} [3]. However, the most interesting region is the transition region between the regime of discrete rotational bands and the regime of compound states, and a detailed microscopic model is required to study the subtle relation between the onset of chaotic motion and the onset of rotational damping. Moreover, it has turned out that simulations of the $\gamma-$decay, based on such a model, can be of considerable help in the difficult task of extracting and interpreting the rich amount of information contained in the experimental γ-ray spectra from the region of the quasicontinuum.

2 The model

We consider deformed nuclei with stable prolate shape. The cranked shell model provides a convenient basis for a detailed description of nuclear rotations and of rotational damping. We then formulate a shell model in which the single-particle basis is represented by the cranked Nilsson orbitals and the intrinsic configurations are represented by many-particle many-hole (np-nh) excitations [4]. An example is shown in Fig. 1, where the proton single-particle levels are shown as a function of rotational frequency. The calculation is performed for the case of ^{168}Yb, using the deformation parameters (ϵ_2, ϵ_4)= (0.255,0.014). We adopt a diabatic basis, removing the interactions at the sharp crossings occurring in the standard cranked shell model, in a way similar to the method followed by Bengtsson [5] (for more details, cf. [6]). In this way the properties of the various configurations display a smooth dependence on frequency. As an example, we select the (0,+) configuration which is yrast at low frequencies. In Fig. 1 we mark by circles the proton orbitals which are occupied in such a configuration at the frequencies $\hbar\omega$= 0.35 and 0.55 MeV. The energy of a configuration $|\mu>$ in the intrinsic frame is given by

$$E'_\mu(\omega) = \sum_{i\in\mu} e'_i(\omega), \tag{1}$$

where the sum is restricted to the orbitals which are occupied in the configuration. The frequency ω corresponds to a value of the projection of the angular momentum on the rotational axis given by

$$J_{x,\mu}(\omega) = \sum_{i\in\mu} j_{x,i}(\omega). \tag{2}$$

In the diabatic basis, the energy of a given configuration changes smoothly as a function of frequency, and locally it is possible to approximate the energy $E_\mu(I)$ in the laboratory frame by [4]

$$E_\mu(I) = E'_\mu(\omega) + \omega I + \frac{(I - J_{x,\mu}(\omega))^2}{2J^{(2)}_\mu} \tag{3}$$

where $J^{(2)}_\mu = dJ_{x,\mu}/d\omega$.

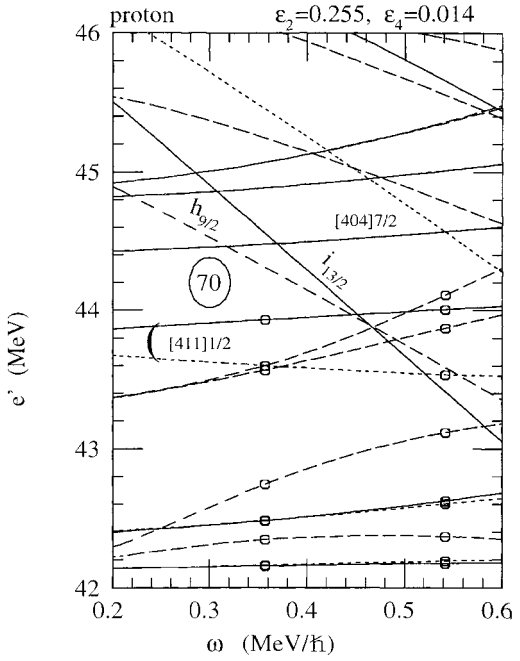

Fig. 1. The cranked single-particle proton levels (routhians) for $^{168}_{70}$Yb are shown as a function of rotational frequency. A circle put on the top of a level at ω = 0.35 and 0.55 MeV/$\hbar$ indicates that the level is occupied in the particular configuration corresponding to the (0,+) band which is yrast at low spin (cf. Fig. 2)

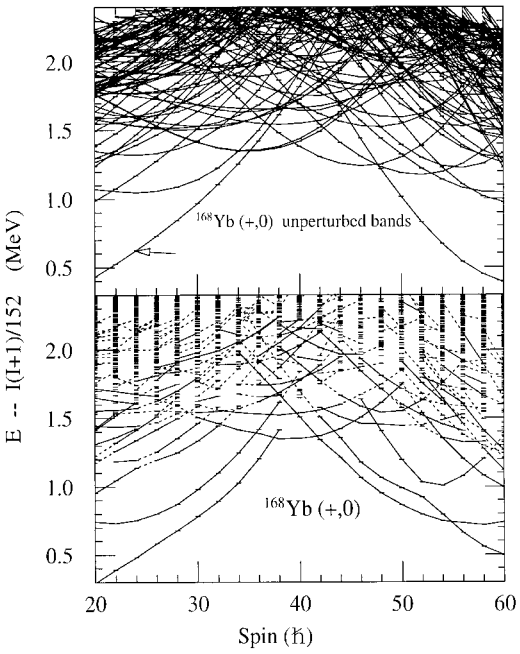

Fig. 2. In the *upper panel*, we show by small horizontal bars the unperturbed energy levels with (+,0) parity and signature at each even spin. Levels based on the same intrinsic np-nh configuration are connected by *solid lines*, producing a set of unperturbed rotational bands. The intrinsic configuration of the yrast band at low spin, marked by the arrow, was shown in Fig. 1. In the *lower panel*, we show the levels obtained diagonalizing the residual interaction. A level at spin I is connected to a level at $I-2$ by a *solid* (*dashed*) line only if the probability $p_{\alpha I\alpha' I-2}$ of the transition, (cf. (7)), is larger than 0.707 (0.5)

The energies of the lowest (+,0) configurations are shown in Fig. 2 (upper panel) as a function of spin. Each intrinsic configuration produces a rotational band. We assume that a state at spin I is connected to a the state at spin $I-2$, based on the same intrinsic configuration $|\mu>$, by a constant E2 transition probability proportional to the square of the quadrupole moment Q_o,

$$B(E2,\mu I\rightarrow\mu' I-2)=\frac{15}{128\pi}Q_o^2\delta_{\mu\mu'}. \tag{4}$$

We then introduce a two-body interaction, V_{2body}, mixing the configurations of given parity and signature. Since the mean-field potential is already included in the Nilsson deformed potential, we subtract the mean field part associated with a reference configuration, denoted by $\mu_{\rm ref}$:

$$V_{res}=V_{2body}-<\mu_{ref}|V_{2body}|\mu_{ref}>. \tag{5}$$

For an even-even nucleus we choose as reference the configuration $\mu_{\rm ref}$ in which the single-particle routhian orbitals are filled up to the Fermi level at low rotational frequency (cf. Fig. 1).

We adopt the surface delta interaction (SDI) [7] as effective two-body force, given by

$$v(1,2)=-4\pi V_o\delta(r_1-R_o)\delta(r_2-R_o)\times\sum_{\lambda\mu}Y^*_{\lambda\mu}(\Omega_1)Y_{\lambda\mu}(\Omega_2). \tag{6}$$

The strength V_o is taken equal to the standard value V_0 = $27.5/A$ [8]. The SDI has been used in the shell model descriptions of nuclei in a wide mass range from light nuclei to deformed rare-earth, providing a reasonable description of the low-lying excitations. It contains the pairing force in the particle-particle channel as well as the multipole-multipole forces in the particle-hole channel.

The energy eigenstates $|\alpha>$ are obtained by numerical diagonalization, and are superpositions of the unperturbed configurations $|\mu>$, $|\alpha(I)>=\sum_\mu X^\alpha_\mu(I)|\mu(I)>$.

The transition probability between mixed states is given by

$$B(E2,\alpha I\rightarrow\alpha' I-2)=\frac{15Q_o^2}{128\pi}\left(\sum_\mu X^\alpha_\mu(I)X^{\alpha'}_\mu(I-2)\right)^2\equiv\frac{15Q_o^2}{128\pi}p_{\alpha I\alpha' I-2}. \tag{7}$$

A measure of the fragmentation of the decay from a given inital state $|\alpha>$ is given by the branching number,

$$n_{branch}(\alpha)=\left(\sum_{\alpha'}p^2_{\alpha I\alpha' I-2}\right)^{-1}. \tag{8}$$

If the decay populates in an uniform way n_f final states, then $n_{branch}=n_f$.

We remark that the matrix elements of the residual interaction are calculated from the cranked orbitals at a given frequency, chosen so that the value of J_x averaged over the intrinsic configurations is equal to I, while the energies of the configurations are obtained by (3). In the diagonalization process we consider the single-particle routhian orbitals located within an interval $\pm$ 3 MeV around the Fermi surface. This space corresponds to 20-30 orbitals for protons and for

neutrons, which generate about 2000-3000 np-nh configurations for each I^π, most of which have 1p1h to 4p4h character. The dimension of the basis is still too large to carry out systematic numerical diagonalizations. To avoid this difficulty, the basis configurations are sorted according to the energy $E_\mu(I) + V(I)_{\mu\mu}$ containing the diagonal residual interaction, and only the lowest 10^3 basis states of a given spin and parity are included in the shell model diagonalization, covering a region of about 2.3 MeV above yrast.

3 Results

As a first result of the model, we show in Fig. 2 (lower panel) the levels resulting from the diagonalization, as a function of spin. Two levels $|\alpha>$ and $|\alpha'>$ at spin I and $I-2$ are connected by a solid line if the associated probability $p_{\alpha I\alpha' I-2}$ is larger than $1/\sqrt{2}$. This assures that $n_{branch}(\alpha) < 2$. For low values of U, the excitation above yrast, we see that there remain sequences of solid lines, building rotational bands as in the unperturbed case. The transition from the region of well-defined rotational bands to the strongly damped rotational motion starts at about 0.8 MeV above yrast and then takes place rather gradually and irregularly, producing strength functions which can differ greatly for neighboring initial states. This can be seen in Fig. 3, where we show the branching number (cf. (8)) as a function of U for the states calculated at two spins and parity. While the increase of the average value of n_{branch} is directly related to the increase in level density, one observes the presence of states with branching numbers not much larger than 2 even at $U \approx 1.5$ MeV.

Similarly, one see from Fig. 2 (bottom) that with increasing values of U there are less and less levels connected by lines, however some can still be found at $U \approx 1.5$ MeV. These short sequences of strong transitions in a region where rotational motion is mostly damped can be appropriately called "scars" of rotational bands [9].

The most specific experimental information concerning rotational correlations in warm nuclei is provided by $\gamma - \gamma$ (and higher fold) coincidences. These spectra display a typical valley-ridge structure, where the ridge is formed by sequences of $\gamma-$rays which follow the energy correlations proper of discrete rotational bands, while the valley is filled mostly by

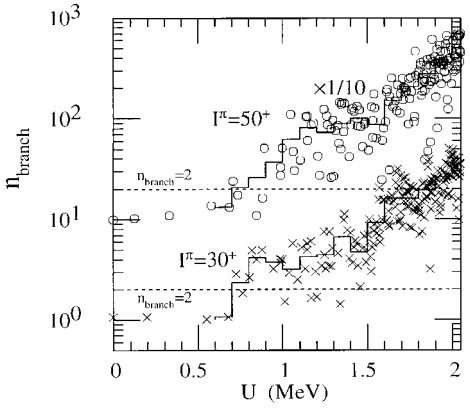

Fig. 3. The branching number of the mixed states $|\alpha>$ at spin and parity I = 30$^+$ and 50$^+$ (multiplied by 10 in the latter case) is shown as a function of U, the excitation energy above yrast

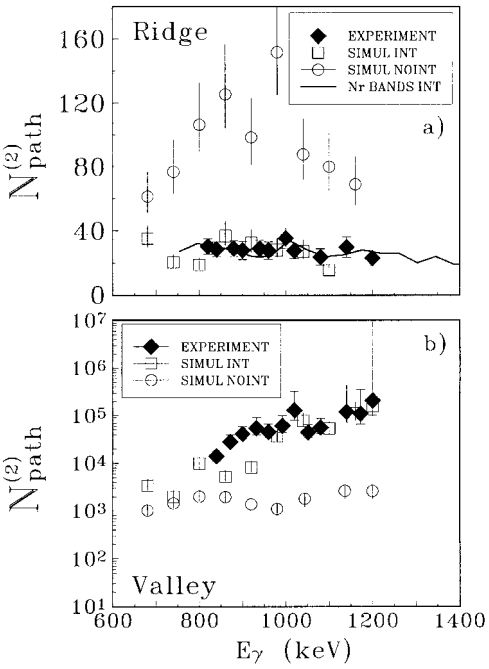

Fig. 4. In the *upper panel*, the effective numbers of paths $N^{(2)}_{path}$ extracted from simulated (*squares*) and experimental (*filled diamonds*) spectra for the nucleus ^{168}Yb are shown, as a function of the transition energy along the first ridge. Also shown by *circles* is the result obtained with non interacting bands. In the lower panel, the same is done along the valley. The *solid line* in the *upper panel* shows the number of strong consecutive transitions at a given spin extracted from Fig. 2 (*lower panel*)

damped rotational transitions. It has been shown [2, 10] that the experimental spectra contain rich quantitative information not only in their intensities, but even more in their fluctuations. A detailed test of the microscopic model can be performed comparing intensities and fluctuations observed in experiment with those produced by the calculated bands. Such properties, however, depend on the level density in the regions sampled by the $\gamma-$cascade in the deexcitation process, and one must combine the microscopically calculated levels and transition strenghts with a good description of the $\gamma-$flow following the fusion-evaporation reaction used to produce the high-spin nucleus. This has been achieved performing Montecarlo calculations which take into account the competition of rotational E2-decay with statistical E1-decay [11]. The region above 2.3 MeV from yrast is described in average, using level densities and rotational damping widths extrapolated from the region below, in which instead microscopically calculated levels and transitions have been introduced in the simulations, producing a finite number of deexcitation paths, which can be followed by the simulated cascade. The fact that these paths are repeatedly followed in the decay process, produces fluctuations in the number of counts in the simulated spectrum.

We have assumed that the strength function of E1-decay is given by the tail of the Giant Dipole Resonance, multiplied by a hindrance factor H_{E1}. We have adopetd the value H_{E1} = 0.09, producing ridge and yrast intensities in overall agreement with the data. This is an important constraint, because it determines to a large extent the regions in spin and excitation energy sampled by the cascade. The effective number of paths $N^{(2)}_{path}$ is obtained from the ratio between the first and second

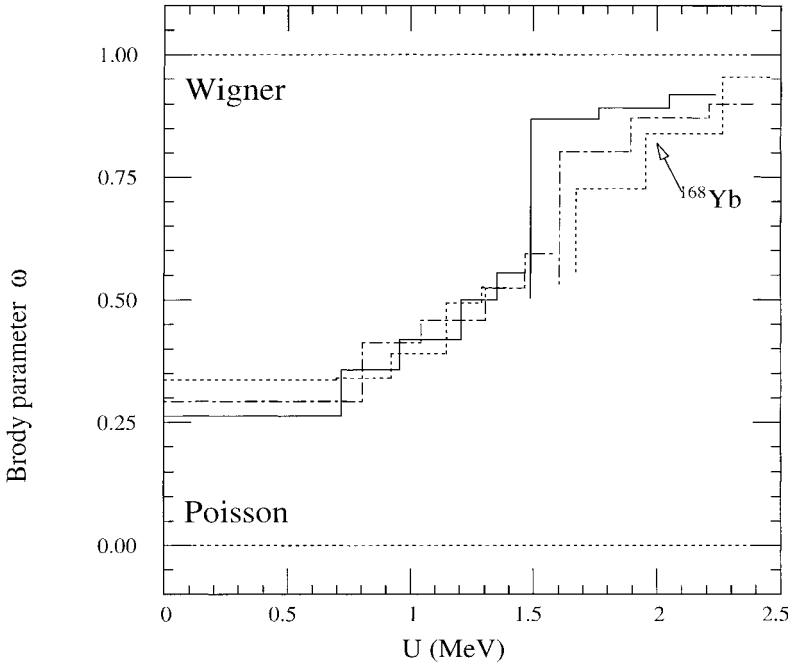

Fig. 5. The Brody parameter extracted from the NNLS distribution for energy bins containing the first to 5-th, 6-th to 10-th, 11-th to 20-th, 21-st to 30th, and 31-st to 40-th levels for each I^π. The result is plotted as a function of average intrinsic excitation energy covered by the bins. The *solid*, *dotted*, and *dot-dashed lines* correspond to different spin intervals $I_0 = 32-50, 20-30, 52-60$ respectively. In order to obtain sufficient statistics, these results have been obtained from calculations performed over 40 nuclei around ^{168}Yb. We also plot the Brody parameter extracted for the higher bins, containing the 51-st to 100-th, 101-st to 200-th, and 201-st to 300-th levels, calculated only in ^{168}Yb

moments of the count fluctuations, according to the equation $\mu_2/\mu_1 = N_{eve}/N_{path} + 1$, where N_{eve} is the number of counts [2, 10]. The number of paths obtained from the simulated and experimental spectra along the first ridge and along the valley are compared in Fig. 4, where it is seen that good agreement is found. If the residual interaction is switched off, the transitions take place along unperturbed rotational bands (cf. Fig. 2, upper panel), producing fluctuations in strong disagreement with the data, as seen in Fig. 4.

The results are sensitive not only to the strength but also to other features of the residual interaction [12]. The damping of rotational motion takes place essentially through the high multipolarities ($\lambda \gtrsim 4$), and they are contained in the surface-delta interaction adopted here. A force like the pairing plus quadrupole interaction with similar values for the average mean square root of the matrix elements produces much less rotational damping, leading to a strong disagreement with the experimental findings.

Until now we have only considered rotational correlations, but the model can also be used to study the properties of energy levels at a given spin. We have found that in the case of ^{168}Yb and in the region with $E - E_{yrast} > 2$ MeV one obtains good agreement with the nearest neighbour level spacing distribution (NNLS) and with the Δ_3 statistics predicted by random matrices theory (GOE) [2, 12]. In the region 0.8-2 MeV where rotational damping sets in and then progressively dominates, the NNLS is intermediate between Poisson and Wigner, gradually approaching Wigner. An example is given in Fig. 4, where we have fitted the NNLS distributions obtained using spacing calculated from 40 nuclei in the region around ^{168}Yb, and fitting the resulting distribution with the so called Brody distribution [13], characterized by a parameter ω which is varied to determine the best agreement with the calculated curve. The Brody distribution reduces to the Wigner (Poisson) limit when ω is equal to 1 (0). A detailed comparison with available experimental data is under way [14].

In the calculations described here, the progressive evolution from the region of rotational bands into the region of rotational damping is accompanied by a transition from Poisson NNLS statistics, typical of ordered motion, to Wigner NNLS statistics, which is a signature of chaotic systems. This, however, may not be necessarily the case. While the existence of a residual interaction capable to mix the simple configurations is needed to induce rotational damping, it is not sufficient, because the mixed bands must also display a sufficient frequency spread Γ_ω. Strong mixing of configurations which react in un uniform way to rotation only gives back well-defined rotational bands. Furthermore, even if Γ_ω is appreciable, when Γ_μ is larger than Γ_ω, one enters the regime of motional narrowing and expects that $\Gamma_{rot} = 2(\Gamma_\omega)^2/\Gamma_\mu$ [3]. The regime of "compound" or "ergodic" rotational bands, in which levels are strongly mixed, but in which Γ_{rot} is smaller than the average level spacing, has been considered recently [15]. It has been suggested that it could appear for nuclei different from those considered here, based on simple estimates of the dependence of Γ_{rot} and Γ_ω on the mass of the nucleus and its deformation. However, no detailed microscopic calculations have been performed so far.

Another issue that has not yet been investigated is the effect of the residual interaction on the low-lying bands, which have been traditionally studied in the cranking model without introducing a residual interaction. In particular, it is an open question whether a model like the one reported here is able to describe quantitatively the band-band interactions which are being found in recent discrete spectroscopy experiments, for example in ^{177}Re and ^{163}Er in which more than 30 and 20 bands have been resolved [16].

References

1. B. Herskind et al.: Nucl. Phys. **557** (1993) 191c
2. T. Døssing et al.: Phys. Rep. **268** (1996) 1

3. B.Lauritzen, T. Døssing and R.A. Broglia, Nucl. Phys. **A457** (1986) 61
4. S. Åberg: Phys. Rev. Lett. **64** (1990) 319
5. T. Bengtsson: Nucl. Phys. **A496** (1989) 56
6. M. Matsuo et al.: to Nucl. Phys. A**6/7** (1997) 1
7. I.M. Green, S. A. Moszkowski: Phys. Rev. **139** (1965) B790; R. Arvieu, S.A. Mozkowski: Phys. Rev. **145** (1966) 830
8. A. Faessler: Fortschr. Phys. **16** (1968) 309
9. R.A. Broglia et al.: Z. Phys. A**356** (1996) 259
10. B. Herskind et al.: Phys. Rev. Lett. **68** (1992) 3008
11. A. Bracco et al.: Phys. Rev. Lett. **76** (1996) 4484
12. M. Matsuo et al.: Phys. Rev. Lett. **70** (1993) 2694
13. T.A. Brody et al.: Rev. Mod. Phys. **53** (1981) 385
14. M. Matsuo et al.: Nucl. Phys. A, in press
15. S.Åberg: Prog. Part. Nucl. Phys. vol.28 (Pergamon 1992) p.11; B.R. Mottelson, Nucl. Phys. **A557** (1993) 717c, and in The Frontier of Nuclear Spectroscopy, eds. Y. Yoshizawa, H. Kusakari and T. Otsuka, World Scientific (1993)7; T. Døssing, Workshop on nuclear structure at finite temperature, Trento 1995, unpublished; S. Åberg, Proceeding of the Workshop on Gammasphere Physics, World Scientific (1996); see also G. Leander, P. Arve and B. Lauritzen, Phys. Rev. **C 37** (1988) 328
16. R.A. Bark et al.: Nucl. Phys. **A591** (1995) 265; A. Brockstedt et al., to be published

This article was processed by the author using the LaTeX style file *pljour2* from Springer-Verlag.